Electronic Supplementary Material (ESI) for RSC Advances.

Supplementary Information

Coupling electric energy and biogas production in anaerobic digesters - impacts on the microbiome

Christin Koch[a], Anne Kuchenbuch[a], Jörg Kretschmar[b], Harald Wedwitschka[b], Jan Liebetrau[b], Susann Müller[a], Falk Harnisch[a]

[a] Helmholtz Centre for Environmental Research – UFZ, Department of Environmental Microbiology, Leipzig, Germany
[b] Deutsches Biomasseforschungszentrum (DBFZ), Department Biochemical Conversion, Leipzig, Germany

Supplementary Methods

Determination of volatile fatty acids

Volatile fatty acids (VFA) concentrations were determined using HPLC. The reactor samples were centrifuged at 20'000 g and 4°C for 10 minutes and filtered with a 0.2 µm nylon filter. They were analyzed with a HPLC (Shimadzu Cooperation, Japan) equipped with a refractive index detector RID-10A and a HiPlex H column 300 x 7.7 mm (Agilent Technolgies, Inc. CA, USA) with a pre-column SecurityGuard Cartidges Carbo-H 4 x 3.0mm (Phenomenex, USA). The liquid phase was 0.01 N sulfuric acid at a flow rate of 0.6 mL min^{-1}, oven temperature was set to 65°C. The samples were run for 60 min isocratically. The following substances were calibrated for their detection: glucose, acetate, lactate, propionate, formate, citrate, succinate, iso-butyrate, iso-valerate, n-valerate, n-butyrate.

Dry matter and organic dry matter determination

Dry matter and organic dry matter were determined in triplicates according to DIN 12880. In detail, dry matter was determined after heating samples in a crucible for 105°C until constant weight. Afterwards, organic dry matter (odm) in these samples was determined by subtraction of the ash content, which was determined after heating the crucible for 30 min at 220°C and then 2 h at 550°C.

PCR cycle parameters

Amplification of the bacterial 16S rRNA gene was performed as described in [1]. For mcrA amplification the PCR cycle parameters were as follows: 1 min at 95°C, 5 initial cycles of 15 s at 95°C, 15 s at 48°C and 30 s at 72°C, including a ramp rate of 0.1°C s^{-1} from the annealing to the extension temperature [2], and 30 cycles of 15 s at 95°C, 15 s at 52°C, and 30 s at 72°C followed by a 20 min extension step at 72°C. Afterwards the PCR products were purified and digested for 1 h with the restriction endonucleases RsaI and HaeIII for 16S rRNA genes and MwoI at 60°C for mcrA (all New England Biolabs, Germany), followed by product precipitation and T-RFLP analysis using an ABI PRISM Genetic Analyzer 3130xl (Applied Biosystems™) and MapMarker® 1000 (BioVentures Inc., USA) for 16S rRNA genes and Red DNA Size Standard (MAC LAB) for mcrA as size standard. Cloning and sequencing was performed as described in [1] and, finally, 96 clones for 16S rRNA of bacteria and 64 clones for archaeal mcrA were investigated for their sequences and terminal restriction fragment (T-RF) length.

Supplementary Figure S1. Complete reactor setup.

The reactor setup is based on modified Automatic Methane Potential Test System (AMPTS, Bioprocess Control AB, Sweden). Here, 15 parallel experiments were performed. The tailor-made glass reactors with the electrodes are standing on magnetic stirring plates within a temperature controlled incubation chamber.

The produced gas from the reactors passes the CO_2 fixing bottles (left hand side of the reactors) and the remaining gas is quantified by the gas volume measuring device as provided by the AMPTS (not in the picture).

Supplementary Figure S2. Acetate spiking test.

After degradation of the volatile fatty acids (day 21, setting I) all reactors were spiked with acetate solution (400 mg L^{-1}). This led to a direct increase in the current density which lasted up to 5 hours indicating that the given amount of acetate was utilized within this time. Considering the coulombic efficiency for acetate utilization (below 1 %) the major acetate utilization has been performed by the methanogenic reactor community.

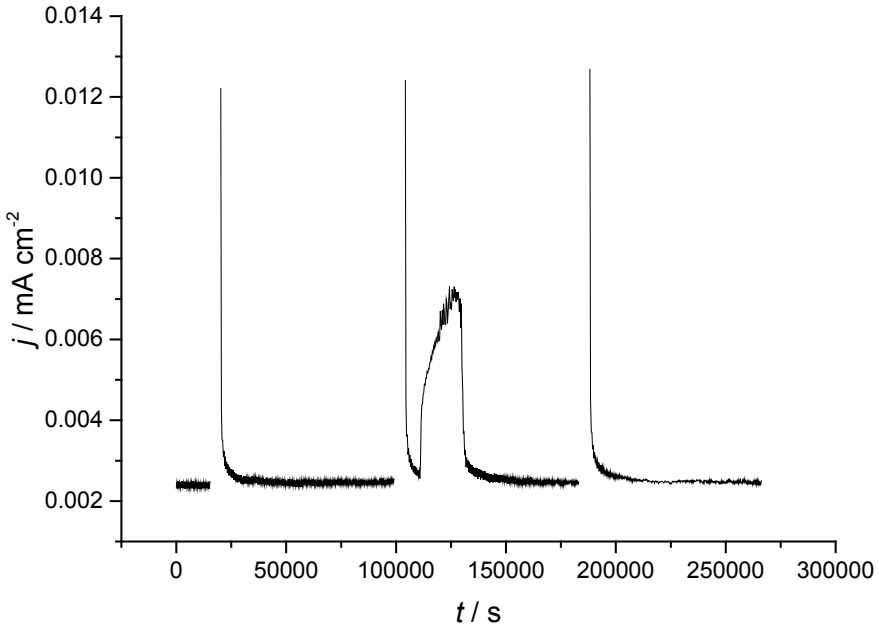

Supplementary Figure S3. Course of substrate degradation and chronoamperograms for experimental setting II.

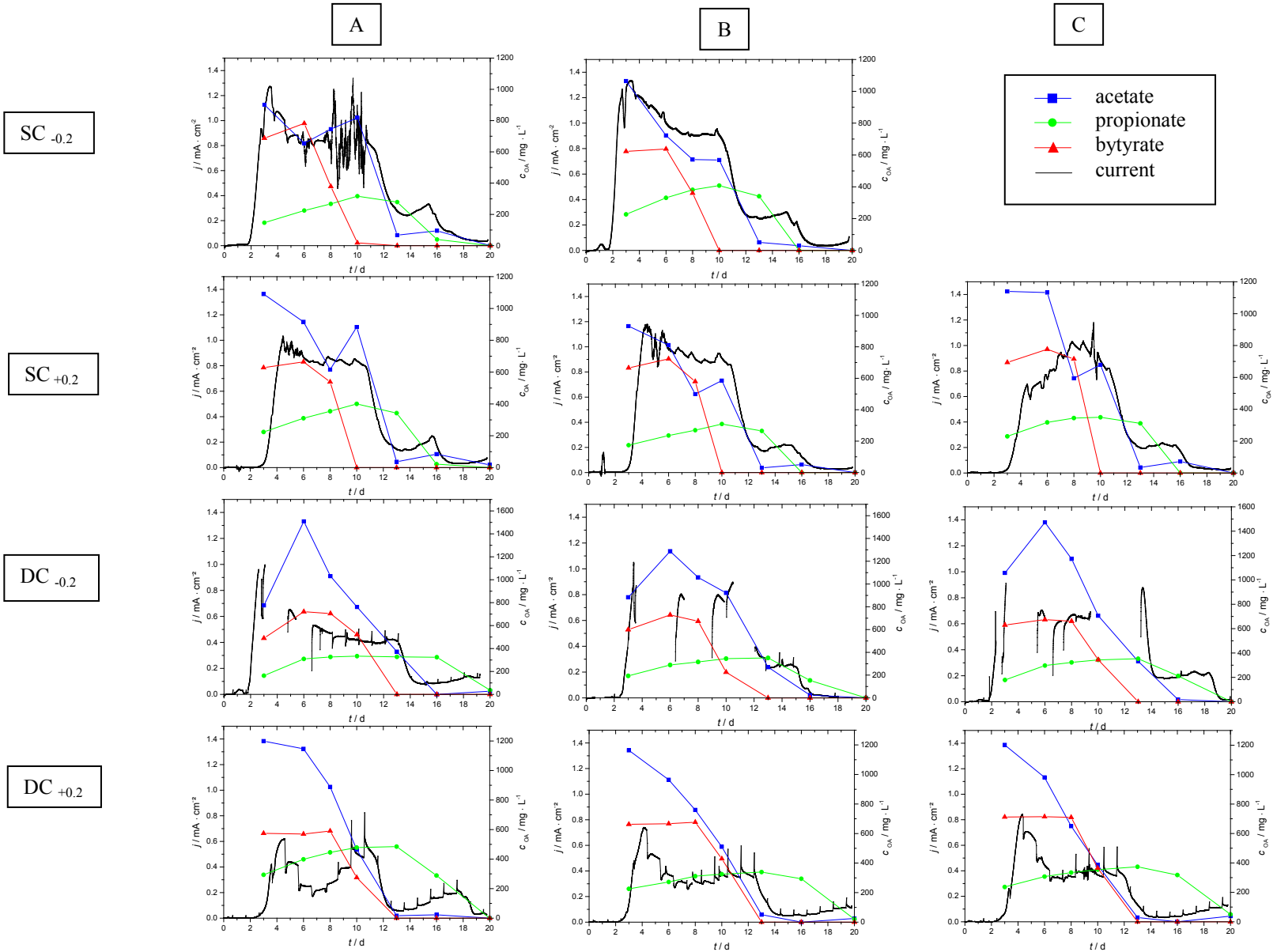

Supplementary Figure S4. Selected CV measurements experimental setting II.
Selected CV measurements of experimental setting II are shown for the early active phase (around the time point of maximum current production) and for the late phase (low current production). A, B and C represent the CVs of the three parallel reactors that were run for each electrochemical setting.

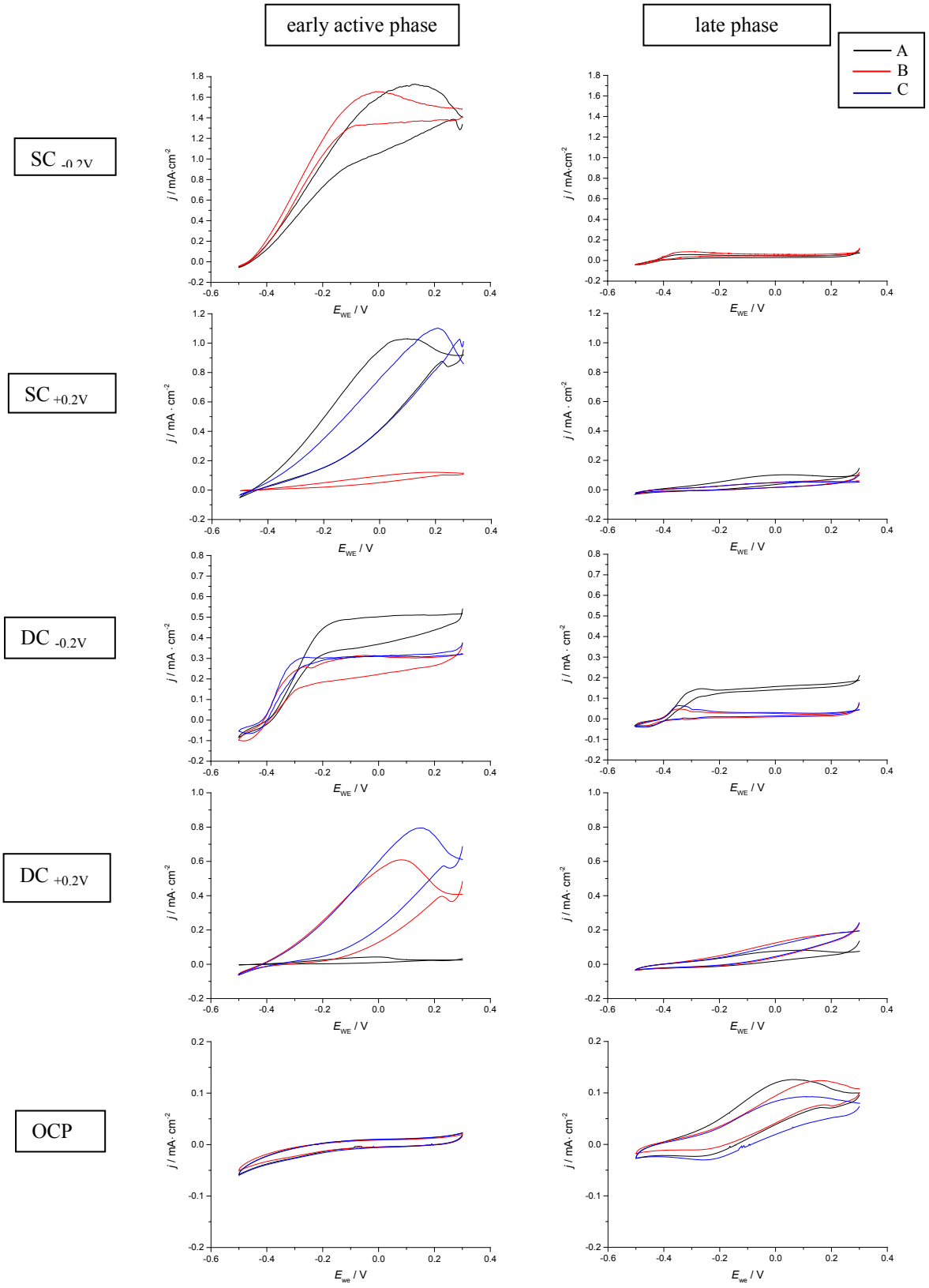

Supplementary Results. Microbial community analysis.

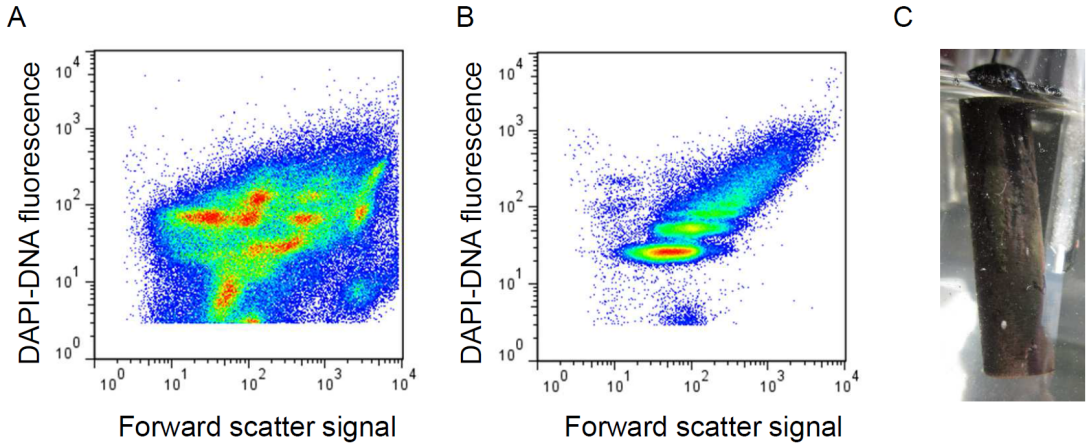

Supplementary Figure S5. Microbial community structure

The microbial community structure of the reactor community and the biofilms was determined with flow cytometry using the cell size related forward scatter signal and DAPI-DNA fluorescence as single cell characteristics. (A) Exemplary cytometric fingerprint of a reactor community showing numerous subcommunities is indicating a high diversity. (B) Exemplary cytometric fingerprint of an anode biofilm sample. Here, only a single phylotype dominates. (C) Exemplary anode biofilm at the end of the experiment. Two coloured layers are visible.

Details T-RFLP results

All in all, 90 different T-RFs were found in the range of 50 to 1000 bp using RsaI for restriction digestion. Five T-RFs were present in all samples (240, 313, 316, 320, 458 bp) and nine T-RFs were in 12 out of 15 reactor samples. The major T-RF of 307 bp in the inoculum samples (37 or 44%) was absent in the reactor communities. There were 28 rare T-RFs that were found in less than four samples. The T-RFs with the highest abundance were 313 bp (8-55% of total peak area), 316 bp (7-18%), 320 bp (4-11%), and 949 bp (3-22%). Three of them can be allocated to groups of *Bacteroidetes* using the clone library. The quite abundant group of *Firmicutes* from the clone library cannot be allocated to single major T-RFs. Here, the high diversity within the *Firmicutes* resulted in the contribution to several smaller T-RFs.

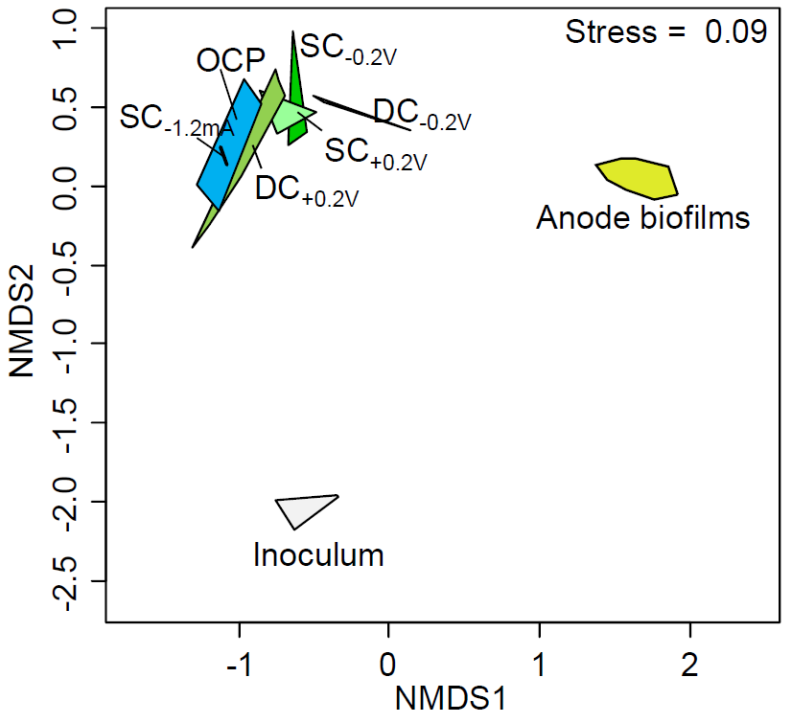

Supplementary Figure S6. Similarity analysis for T-RFLP results.

Community composition in setting II and III: The T-RFLP results for the end point samples of the reactor community and the anode biofilms of all experiments with setting II and III are arranged regarding their similarity (non-metric multidimensional scaling, NMDS). The parallels of the reactor samples of each setup ($SC_{-0.2V}$, $SC_{+0.2V}$, $DC_{-0.2V}$, $DC_{-0.2V}$, $SC_{-1.2mA}$ and AD control (OCP)), the inoculum and all biofilm samples are indicated.

Methanogenic community

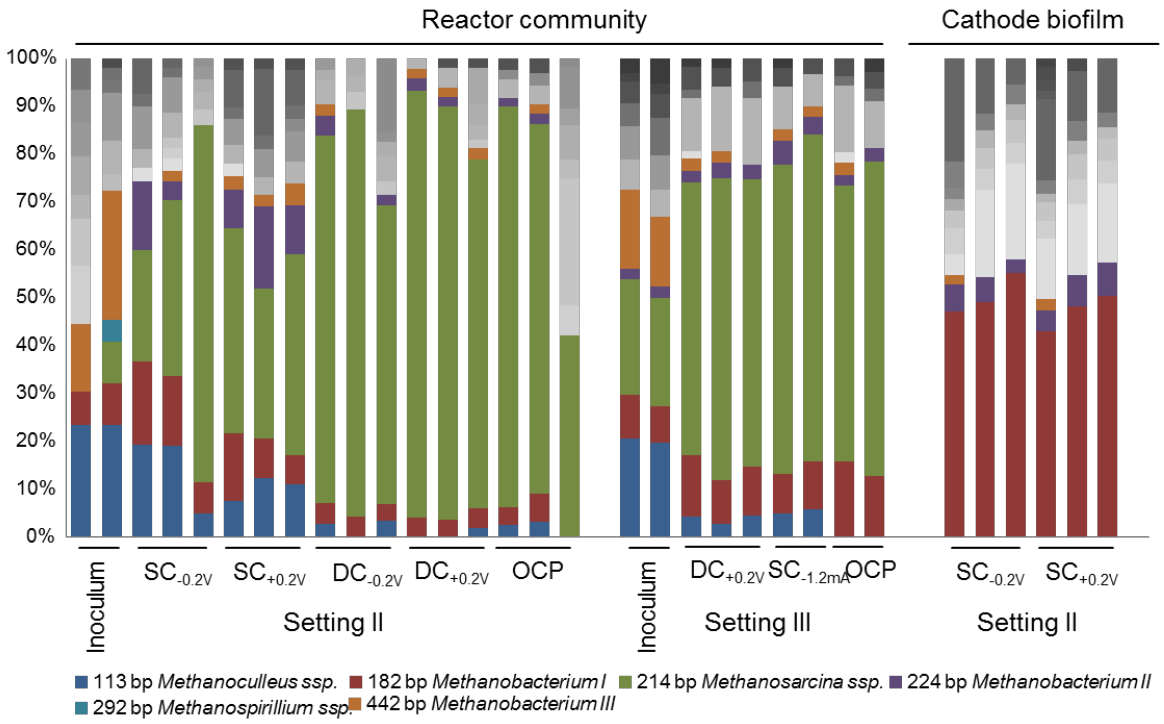

Supplementary Figure S7. Methanogenic community composition.

Under the experimental settings II and III the methanogenic community was dominated by typical methanogenic representatives of the anaerobic digestion process [3]. The T-RFLP results were dominated by a T-RF that was assigned to the genus *Methanosarcina* (23-89%). Compared to the inoculum this group increased its abundance in all reactors. Other T-RFs were assigned to *Methanoculleus* spp. and three groups of *Methanobacterium* spp.. The T-RF of *Methanoculleus* spp. was more abundant in the SC electrochemical setups (8-19%) compared to the DC and OCP control (0-3%). The same trend was found for *Methanobacterium* I with 6-17% in the SC setup and 0-6% in the DC reactor and OCP control. Unidentified T-RFs are indicated in grey.

The DNA extracts from the working electrodes only gave a weak PCR amplification product and the resulting T-RFLP results were very similar to the reactor community (not shown). Therefore, it is supposed that there was no specific enrichment of methanogenic organisms on the working electrodes.

A B

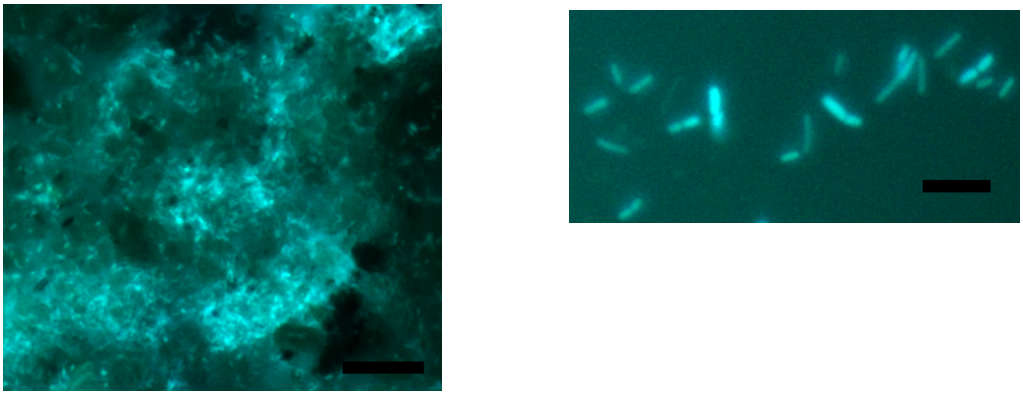

Supplementary Figure S8. Microscopic image of cathodic biofilm.

Interestingly, the methanogenic community of the unshielded counter electrodes was mainly represented by *Methanobacterium* I. Fluorescence microscopic observation of the counter electrode biofilms (fresh biofilm samples from the single-chamber setup were scratched off the cathodes, prepared on a microscopy slide and analyzed with Axioplan-2-Imaging (Zeiss, Germany) using the filter set 05 (BP 395-440, FT 460, LP 470) for detecting methanogenic autofluorescence) revealed a homogenous biofilm consisting of bright autofluorescent cells which is typical for methanogenic archaea. It is therefore concluded that a specific enrichment of archaea on the counter electrode took place. (A) Scale bar 50 µm. (B) Scale bar 5 µm.

Supplementary Table S1. Raw data methane production.

The raw data of the AMPTS gas volume measuring device is given in the following tables in mL CH_4 g_{odm}^{-1}. Apparent outliers were not considered for calculating the average methane production per experimental setup. They are most probably caused by small leakages in the reactor setup. The total gas volume was corrected for the methane potential of the inoculum (only experimental run I), for added buffer volumes during rinsing the lugging capillary after being clogged and added gas volumes for testing the leak tightness of the systems.

a) Experimental Run I

Day	$SC_{-0.2}$			$SC_{+0.2}$			$DC_{-0.2}$			$DC_{+0.2}$			AD control (OCP)								Inoculum		
0	0	0	0	0	0	0	0	0	0	0	0	0	0	0	0	0	0	0	0	0	0	0	0
1	107	90	122	116	121	118	125	120	63	119	1	122	2	51	114	12	13	13	101	2	7	7	7
2	149	164	214	207	207	210	214	215	67	212	16	216	4	104	205	68	70	69	165	180	8	7	7
3		234	282	275	208	278	310	281	68	281	23	287	5	167	266	81	84	82	237	252	9	8	8
4		258	306	297	208	302	344	307	69	306	25	313	5	191	267	95	99	98	288	304	10	8	8
5		275	322	305	209	318	365	325	77	323	26	331	6	208	268	115	120	119	318	334	11	9	9
6		287	333	323	209	330	383	338	90	336	33	347	6	223	270	145	152	149	339	354	13	10	10
7		296	342	331	210	338	396	349	98	346	34	357	6	232	272	186	194	191	354	369	14	11	12
8		304	349	337	211	347	406	357	104	367	37	365	6	233	277	236	245	241		369	16	13	14
9		309	353	344	211	350	413	362	108	373	44	370	6	234	278	287	294	290		370	17	14	16
10		312	357	345		350	420	366	109	378	45	373	7	235	279	308	312	312		370	19	14	18
11		314	358	346		351	423	368	110	381	46	376	7	235	280	315	318	321			20	15	19
12		315	359	347		351	426	371	110	382	46	378	7	236	281	321	322	326			21	15	20
13		318	361	348		351	430	373	110	384	47	380	7	236	283	326	328	331			22	16	21
14		320	365	349		351	432	374	111	385	47	382	8	237	285	331	334	336			23	16	23
15		322	367	349		352	434	374	111	386	48	382	8	237	286	338	338	340			24	17	24
16		323	368	350		352	437	375	111	386	48	383	8	238	287	342	342	343			24	17	
17		324	369	350		352	438	375	112	387		383	9	238	287	345	347	345			25	18	
18		325	370	351		353	438	376	112	387		384	9	239	288	348	349	347			26	18	
19		325	371	351		353	439	376	112	388		384	10	239	288	350		349			26	19	
20		326	371	352		353	440	377	112	389		385	10	239	289			350				19	
21		331	380	355		354	448	381	116	393		389	18	247	293								
22				356									21	251									
23														255									
Total volume	149	331	380	356	211	354	448	381	116	393	48	389	21	255	293	350	349	350	354	370	26	19	24
Outlier excluded		331	380	356		354	448	381		393		389			293	350	349	350	354	370	26	19	24
Corrected volume		298	347	293		321	365	318		330		346			270	327	326	327	331	347	26	19	24

b) Experimental Run II

Day	$SC_{-0.2}$			$SC_{+0.2}$			$DC_{-0.2}$			$DC_{+0.2}$			AD control (OCP)								
0	0	0	0	0	0	0	0	0	0	0	0	0	0	0	0	0	0	0	0	0	0
1	66	1	0	40	1		31	57		20	34	25	15	5		6	0	0	1	17	14
2	79	2	1	60	1		67	67		67	73	65	57	27		6	1	1	46	47	48
3	81	3	1	61	2		73	68		68	74	67	57	29		7	1	1	48	49	49
4	85	9	2	64	2		78	69		72	84	71	58	31		7	2	2	50	51	50
5	101	23	2	78	6		87	74		92	102	93	59	39		8	2	2	50	55	51
6	119	41	3	97	14		100	84		107	113	108	62	46		14	11	8	51	59	55
7	133	56	11	116	19		108	97		117	122	119	70	47		31	25	22	54	68	57
8	161	78	23	136	32		118	110		127	132	129	79	52		33	29	28	56	80	67
9	183	100	40	164	39		122	131		141	143	141	91	69		36	32	30	59	97	89
10	203	120	59	189	45		129	148		164	158	157	113	94		42	35	34	65	120	115
11	220	136	76	210	48		144	167		188	176	174	142	124		51	40	39	74	150	141
12	234	144	78	221	55		159	180		202	193	188	172	148		67	48	46	88	176	166
13	243	152		225	57		174	190		203	205	193	192	162		88	60	62	106	200	193
14	250	162		230	64		188	196		204	208	193	206	170		114	78	84	129	212	209
15	259	173		238	72		191	202		204	208	194	213	176		144	106	113	155	217	218
16	266	180		247	74		192	212		205	209	194	220	186		169	137	146	183	224	230
17							193	215		209	210	195	230	197		184	159	176	208	239	245
18							193			217	210	195	235	199		192	169	190	222	259	262
19							194				211	196				200	174	195	228	261	266
20																213	175	199	236		
Total volume	266	180	78	247	74	0	194	215	0	217	211	196	235	199	0	213	175	199	236	261	266
Outlier excluded	266	180		247			194	215		217	211	196	235	199		213	175	199	236	261	266
Corrected volume	266	180		247			194	215		217	211	196	235	199		203	165	189	226	251	256

Supplementary Table S2. Corn silage characteristics.

The corn silage composition was limited to C, O, and H as major carbohydrate constituents and the sum formula determined based on the general composition of corn silage as described in [4] leading to the sum formula $C_{22}H_{36}O_{18}$. For simplification nitrogen and sulfur (protein components) were not explicitly considered. Proteins contribute similarly to the biogas production as carbohydrates and represent about 8.5% of the dry matter (DM). The contribution of fat is insignificant as this fraction was found to be about 2% of the DM. Average values of corn silage as used in the current experiment (based on standard animal feed analysis performed at Deutsches Biomasseforschungszentrum (DBFZ)).

Fraction						**g kg_{DM}^{-1}**
Carbohydrates	Crude fiber					233.3
	Nitrogen free extracts					619.0
Dry matter (DM)	Ash					43.6
	Organic dry matter (ODM)	Crude protein				84.6
		Crude fat				19.5
		Carbohydrates	Nonfiber carbohydrates (NFC)			253.5
			Neutral detergent fiber (NDF)	Acid detergent fiber (ADF)	Celllulose	226.5
					Lignin	46.2
				Hemicellulose		326.0
Neutral detergent fiber (NDF)						598.7
Acid detergent fiber (ADF)						272.7

References

1. Koch, C., Popiel, D., Harnisch, F. 2014. *ChemElectroChem*, **1**(11), 1923-1931.
2. Steinberg, L.M., Regan, J.M. 2008. *Applied and Environmental Microbiology*, **74**(21), 6663-6671.
3. Demirel, B., Scherer, P. 2008. *Reviews in Environmental Science and Bio/Technology*, **7**(2), 173-190.
4. Weissbach, F. 2009. *Pflanzenbauwissenschaften*, **13**(2), 72-85.